The influence of nanotexturing of poly(lactic-co-glycolic acid) films upon human ovarian cancer cell attachment

Gökçen Yaşayan[1,2], Xuan Xue[1], Pamela Collier[3], Philip Clarke[3], Morgan R Alexander[4] and Maria Marlow[1]*

1. University of Nottingham, School of Pharmacy, Division of Drug Delivery and Tissue Engineering, Boots Science Building, University Park, Nottingham, NG7 2RD, UK
2. Marmara University, Faculty of Pharmacy, Department of Pharmaceutical Technology İstanbul, 34668, Turkey
3. University of Nottingham, School of Medicine, Division of Cancer and Stem Cells, Nottingham, NG7 2UH, UK
4. University of Nottingham, School of Pharmacy, Laboratory of Biophysics and Surface Analysis, Boots Science Building, University Park, Nottingham, NG7 2RD, UK

KEYWORDS Nanotexturing, human ovarian cancer cell, poly(lactic-co-glycolic acid), films

ABSTRACT In this study, we have produced nanotextured poly(lactic-co-glycolic acid) (PLGA) films by using polystyrene (PS) particles as a template to make a polydimethylsiloxane (PDMS) mold against which PLGA is solvent cast. Biocompatible, biodegradable and nanotextured PLGA films were prepared with PS particles of diameter of 57, 99, 210, and 280 nm that produced domes of the same dimension in the PLGA surface. The effect of the particulate monolayer templating method was investigated to enable preparation of the films with uniformly ordered surface nanodomes.

Cell attachment of a human ovarian cancer cell line (OVCAR3) alone and co-cultured with mesenchymal stem cells (MSC) was evaluated on flat and topographically nano-patterned surfaces. Cell numbers were observed to increase on the nanotextured surfaces compared to non-textured surfaces both with OVCAR3 cultures and OVCAR3-MSC co-cultures at 24 and 48 hour time points.

INTRODUCTION

Nanotexturing of biomaterials has been widely used to mimic the extracellular matrix and is currently an approach used to modulate, isolate and optimize the response of the cells for multiple applications in regenerative medicine and cancer therapeutics. (Zhang and Webster 2012)

Previous studies of the topographical influence of cell-material attachment have been carried out with geometries including grooves, wells, pits, and protrusions on a diverse range of materials. The results for mature cells including cancer cells show that they respond to nano- and micro-textured biomaterial surfaces, where changes in cell adhesion, proliferation, orientation, alignment, migration and morphology were all observed. (Curtis and Wilkinson 1997, Sarna *et al* 2009, Flemming *et al* 1999, Andersson *et al* 2003, Matsuzaka *et al* 2003, Recknor *et al* 2004, Miller *et al* 2007, Falconnet *et al* 2006, Martinez *et al* 2009, Lamers *et al* 2010, Zhang and Webster 2012, Hsu *et al* 2005) These textured biomaterials may mimic *in vivo* microenvironments, and thus enable modelling of cell-cell and cell-extracellular matrix interactions and modulation of cell-surface interactions. (Ng *et al* 2012, Craighead *et al* 1998, Martinez *et al* 2009, Dalby *et al* 2004)

Although there are numerous studies on textured materials, the complexity of their role in controlling cell interactions and cell responses is still yet not fully understood and hence is

impossible to predict without carrying out the individual cell studies. Also the response mechanisms of different cell lines to textured surfaces are not well defined. (Zhang and Webster 2012, Andersson *et al* 2003, Lamers *et al* 2010, Miller *et al* 2007, Martinez *et al* 2009, Hsu *et al* 2005) Hence in this study, we have focused on fabrication, characterization and cell culture studies of hemispherical protrusions to provide nanotextured biodegradable biomaterials to characterize the ovarian cancer cell response to this surface topography. We have focused on fabrication of large scale (1 cm x 1 cm), defect-free textured surfaces with various protrusion dimensions, and their impact on ovarian cancer cell attachment.

Hemispherical protrusion shaped nanotextured materials were manufactured using a colloidal particle lithography technique employing polystyrene (PS) particles with the diameters from 57 to 280 nm. The PS templates were prepared by using two methods, the first as described in Zhang and Webster's study (Zhang and Webster 2012) which enabled formation of a multi-layered templates, and a second approach (Ogaki *et al* 2010) by using self-assembly of PS particles at an air-water interface which produced mono-layered particles reducing the occurrence of step edges in the nano imprinted polymer surfaces. The latter method has not been used before to prepare biomaterial surfaces. The PS templates were used to form a negative relief in polydimethylsiloxane (PDMS) from which replication of the particulate topography was obtained in the biodegradable poly(lactic-co-glycolic acid) (PLGA) films (Figure 1).

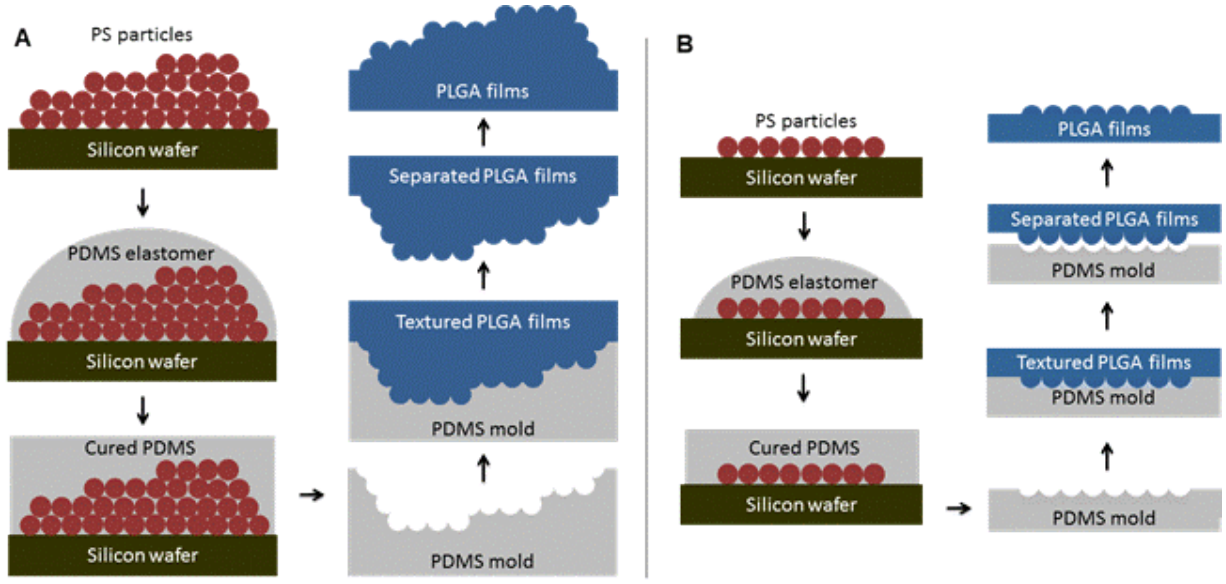

Figure 1. A schematic representation for preparation of the PLGA films. Surface morphologies of the PS particles were transferred to PDMS templates as inverse molds. By using PDMS molds, PLGA films were obtained. A. Preparation of **multi-layered** PLGA films. With this method, step edges on the surface between areas of disorder were observed. B. Preparation of **mono-layered** PLGA films. With this method, no other surface morphology was observed other than nanotexturing.

Atomic force microscopy (AFM) was used to characterize the topography, X-ray photoelectron spectroscopy (XPS) to analyze surface chemistry, and contact angle to measure the surface wettability.

Cell attachment on PLGA films was evaluated with an ovarian cancer cell line, OVCAR3, and OVCAR3 co-cultured with MSC. Specifically, the cell responses to non-textured PLGA films and nanotextured PLGA films were compared. With ovarian and other cancer types, the presence of a viable stem cell niche i.e. MSCs is critical to tumor growth and invasion, conferring a metastatic phenotype and chemo- and radio-resistance. Indeed, co-culturing the OVCAR3's with MSC's provides more disease relevance and appropriate cell:cell interactions. Specifically MCS's will differentiate into fibroblasts, thereby providing increased opportunity for cancer cell anchorage. (Touboul *et al* 2013, Lehmann *et al* 2011, Haller *et al* 2000)

Materials and methods

Preparation of polystyrene (PS) templates

a) Multi-layer PS templates Multi-layer PS templates were prepared as described previously (Zhang and Webster 2012, Carpenter *et al* 2008); borosilicate glass coverslips (18 mm in diameter, Fisher) were cleaned and degreased by acetone, ethanol (70%) and dH_2O. Then PS suspensions (300 μL, 10wt%, Bangs Labs) with the diameters of 57 nm, 99 nm, 210 nm or 280 nm were pipetted onto the coverslips, and vacuum desiccated to remove the solvent (~2 days).

b) Mono-layer PS templates Mono-layer PS templates were prepared as described previously (Rybczynski *et al* 2003, Ogaki *et al* 2010). Silicon wafers (Sigma-Aldrich) were cut to small (~1 x 1 cm^2) and large (~1 x 3 cm^2) sizes and sonicated with ethanol. Afterwards they were washed several times with Milli-Q water (Millipore, resistibility of 18.2 MΩ cm^{-1} at 25 °C), and blown dry with nitrogen at room temperature. After drying, the silicon wafers were exposed to UV to increase wafer hydrophilicity for 20 minutes (UV/Ozone ProCleaner, BioForce Nanosciences, Inc.). The large silicon wafer was placed in a petri dish at an inclined plane, and the Petri dish was filled with Milli-Q water. PS particle suspension (100 μL, 10 wt%) was mixed with an equal amount of ethanol. This mixture was applied slowly over the large silicon wafer to water surface using an Eppendorf pipette, the silicon wafer was then slowly submerged in the water. To obtain hexagonal close packed particles, a dodecylsodiumsulfate (SDS) solution (2%, ~10 μL) was added to Petri dish. The PS mono-layers on the water-air interface were then lifted off from the water surface by using the small-size silicon wafer, and were dried at room temperature. The surfaces were prepared by using PS particles with the diameters of 99 nm, 210 nm or 280 nm.

Preparation of poly(dimethysiloxane) (PDMS) templates PDMS (Sylgard 184 silicone elastomer, Dow Corning) was mixed thoroughly (curing agent: base, 3.5 mL: 26.5 mL), and then centrifuged for 15 min at 2000 rpm. It was poured over the PS coated coverslips (or silicon wafers) placed in a borosilicate glass Petri dish, residual bubbles were removed by vacuum extraction and the wafer was heated to 40 °C for 2 h to accelerate the curing process. Once cooled, the PDMS template was separated from PS template. The PDMS template was washed with acetone to remove the remaining PS particles on the surface.

Preparation of poly(lactic-co-glycolic acid) (PLGA) films

PLGA (1g, 50:50 PLA/PGA, 7000-17000; Sigma Aldrich) was dissolved in chloroform (10 mL), and poured over the PDMS molds, then placed into a vacuum desiccator to avoid bubble formation. After allowing evaporation of the solvent for 48 h, PLGA films were peeled off from the molds and placed on glass coverslips. To remove the residual PDMS, PLGA films were washed with hexane (Sigma-Aldrich). For control studies, non-textured PDMS and PLGA films were prepared without PS beads following the procedure described above.

AFM studies

Topography images and analysis (section and bearing) of PS, PDMS and PLGA films were obtained in air using a D3000 Atomic force microscopy (AFM) instrument with a NanoScope IIIa controller (Bruker) operating in Tapping™ mode. RTESPA AFM probes (nominal resonant mechanical frequency: 300 kHz, spring constant: 40 N/m, Bruker) were used, and images were acquired using an E-scanner, at scan rates between 0.6-1 Hz, with a resolution of 512 x 512 pixels. Image data was analyzed, section and bearing analysis were carried by NanoScope Analysis software-Version 1.20 (Bruker).

Optical microscopy studies

The samples were viewed using an optical microscope (Prior Scientific Instruments Ltd.) equipped with a digital camera (QICAM Fast 1394, QImaging).

Water contact angle measurements

Water contact angle measurements of the films were measured by a Krüss DSA 100 instrument by dispersing an ultrapure Milli-Q water droplet (Millipore, resistibility of 18.2 MΩ cm^{-1} at 25 °C) with a volume of ~400 pL.

X-ray photoelectron spectroscopy (XPS) measurements

The samples were analyzed using XPS in order to determine surface elemental composition using a Kratos AXIS Ultra Spectrometer (Kratos Analytical, Manchester, UK) with a mono-chromatic Al Kα X-ray source (1486.6 eV) operated at 10 mA emission current and 12 kV anode potential. The ULTRA was used in fixed analyzed transmission (FAT) mode, a pass energy of 80 eV was used for the wide scans, and 20 eV for the high resolution scans. Data analysis was carried out using CASAXPS software with empirically derived sensitivity factors to determine the composition (atomic percent) from the peak areas. The photoelectrons were collected normal to the sample surface. The measurements were carried only with a mono-layer textured 280 nm films and non-textured films which had been cast against a flat PDMS mold.

The residual PDMS layer thickness over the mono-layered 280 nm textured PLGA films and the non-textured films were calculated by using the silicon signal in the XPS data. Topofactors for hemispheres were used to calculate the equivalent conformal PDMS thickness of the textured surfaces. (Shard *et al* 2009, Shard 2012)

Human ovarian carcinoma cell and mesenchymal stem cell adhesion assay

Human ovarian carcinoma cell line, OVCAR3 (US National Cancer Institute) was cultured only/or co-cultured with mesenchymal stem cell line, hm-MSC-bm (Sciencell Research

Laboratories, CA, US) in Dulbecco's modified eagles medium (DMEM, Sigma, UK) with 10% Fetal bovine serum (FBS, Sigma, UK).

For sterilization of the films, PLGA films were removed from the coverslips by soaking in 70% ethanol for approximately 4 hours, and later soaking in clean 70% ethanol for approximately 20 minutes. The surfaces were sterilized by UV light for 5 minutes in ethanol, and later 5 minutes, without ethanol. After rinsing with media the films were placed in 3 ml of DMEM + 10% FBS.

OVCAR3 cells were labelled with Cell tracker^{TM} CM-DiI red fluorescent protein reporter (Life Technologies, UK) and cultured on three different surfaces including a control well of a 6 well plate (flat plastic), non-textured PLGA films, and textured PLGA films prepared from mono-layered 280 nm PS templates for 48 hours. For each condition the cells were plated (OVCAR3 only, OVCAR3 and MSC's combined at a 1:1 ratio) on duplicate wafers (one per well, six well plates) with a final density of 6×10^5 and monitored over 48 hours for cell adhesion. 3 plates, one for each time point were set up (4, 24 and 48 hours) and in each case the wafers were removed for counting.

At 4, 24 and 48 hours, the cells in all conditions were counted manually over 3 regions of interest for each duplicate well where possible. Cells emitting red light were photographed at 10X objective magnification in 3 areas of each well (duplicate wells). Each image was divided into 4 equal (dimensions) Regions of Interest (ROI's) and the cells counted. In this study, number of cells attached to the films at the 4 th hour, 24th hour, and 48th hour were studied.

Statistical analysis

The validation and analysis of cell attachment data was carried out in SPSS 21, (IBM) using Wilcoxon signed ranks test. Other statistical analysis was performed by a two sample t-test assuming both equal and unequal variances. Statistical significance was accepted at $p < 0.05$.

RESULTS

In these studies we have focused on fabricating regular nanotextured and defect-free materials over large lengths scales compatible with the cell culture experiments (1 cm x 1 cm).

Nanotextured surfaces prepared from multi-layer PS templates

Utilizing the Zhang and Webster method (Zhang and Webster 2012), we successfully produced PDMS templates from multi-layers of PS spheres. Using AFM imaging, we determined that the form of the PS templates were transferred to PDMS templates and then to the PLGA films (Figure 2). This data also indicated that the diameters of the features in PS templates and PLGA films remained unchanged during the fabrication process of the films. (See also Figure S3, ESI).

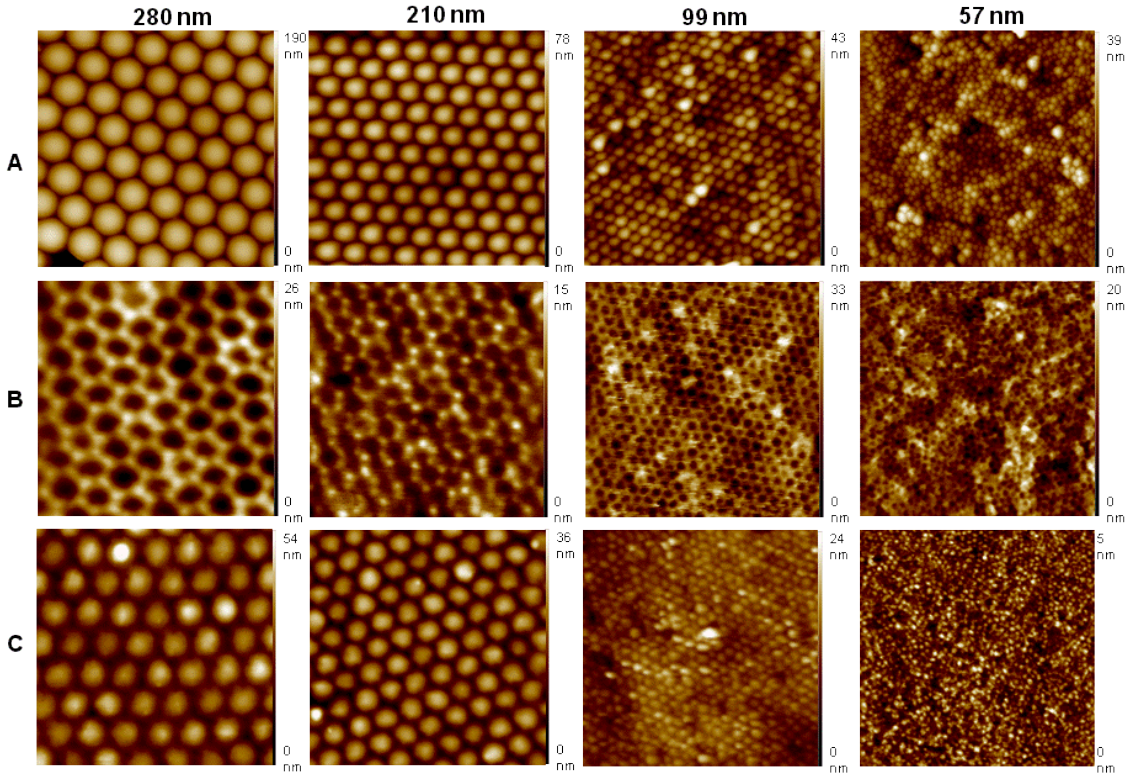

Figure 2. AFM topography images of PS surfaces (A), PDMS surfaces (B), and PLGA films (C) prepared from multi-layer PS templates. The surfaces were prepared by use of 280 nm, 210 nm, 99 nm, and 57 nm PS beads. All images were 2 μm x 2 μm.

From the AFM images of the PS particles, the PDMS mold and the PLGA surfaces presented in Figure 2, hexagonal close packing of the particles is evident for the 210 and 280 nm assemblies, but this was accompanied by retention of PS particles in the structure imprinted in to the silicone mold for the 99 nm surface and the order was not present in the 57 nm beads.

AFM studies with larger scan areas (8 μm x 8 μm) indicated the presence of flat layers of particles, separated by step edges between areas of disorder in the PLGA films (Figure 3). These step edges were attributed to the formation of multi-layers during PS template preparation (Figure S4, ESI). By analysis of the AFM images, the percentage of the protrusions by boundary structures in the PDMS surfaces was found to be up to ~7% of the overall scan area.

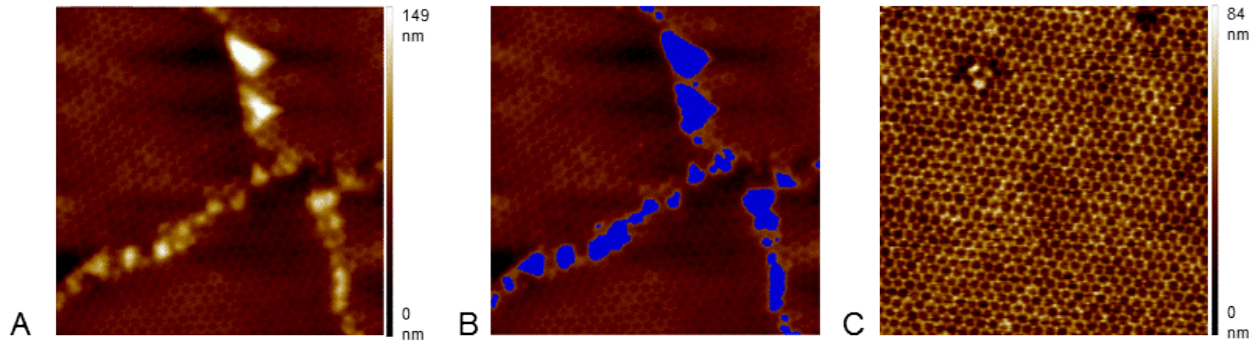

Figure 3. Representative AFM images of multi-layered and mono-layered silicone mold surfaces. For multilayered surfaces (A), surface irregularities on the surface were observed. For the PDMS surfaces prepared from 280 nm multi-layer templates, the area occupied by boundary structures (B, the area in blue) was 7.1%. No boundary structures were observed for the PDMS surfaces prepared from 280 nm mono-layer templates (C). 8 μm x 8 μm scan.

Nanotextured surfaces prepared from mono-layer PS templates

In an alternative method, adapted from Ogaki et al (Ogaki *et al* 2010), PS templates were prepared by self-assembly of the PS beads on the water-air interface; a single layer of PS particles were spread on the wafer during the preparation of the templates. Mono-layered PS

templates were prepared from beads with the diameters of 280 nm, 210 nm and 99 nm, but 57 nm particles did not prove effective. (Figure S5, ESI) For the templates prepared from 280 nm and 210 nm, AFM results indicated that PS mono-layer templates were prepared successfully, without the retained particles as found in the multilayer molding, and the nanotexturing was again transferred to PDMS and PLGA films. For 99 nm templates prepared by this new method, multi-layers were observed and surface regularity was disrupted compared to larger particle diameters. (Figure 4) For 210 nm and 280 nm PS particles, step edges were not observed on the surfaces (Figure S6, ESI). Optical microscopy images have also confirmed the elimination of the macroscopic defects (Figure S7).

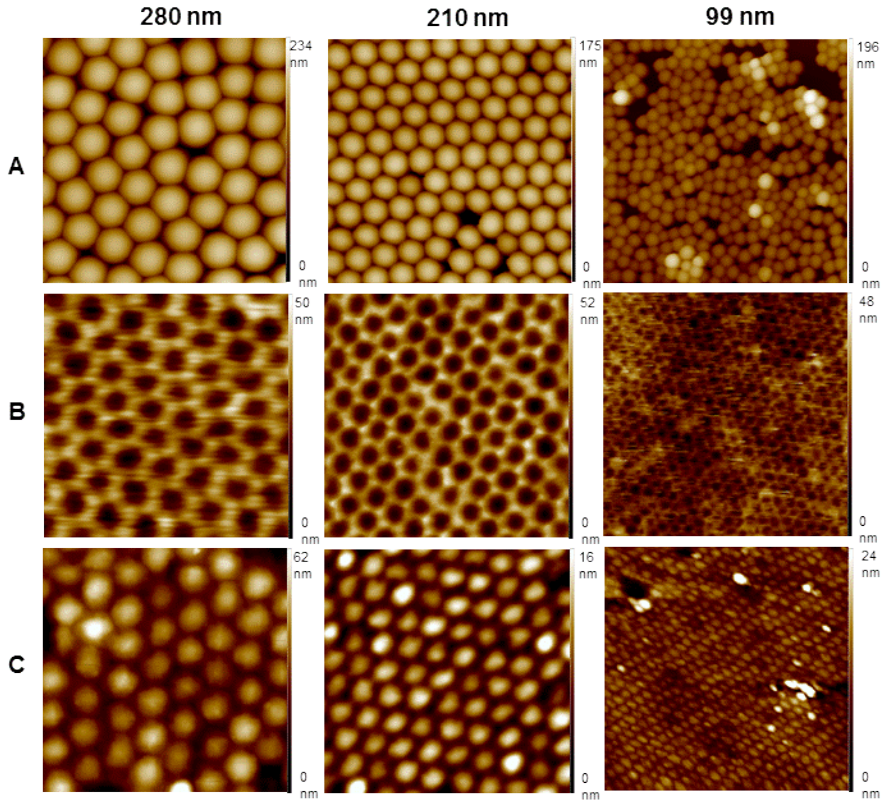

Figure 4. AFM topography images of PS surfaces (A), PDMS surfaces (B), and PLGA films (C) prepared from mono-layered PS templates. The surfaces were prepared by use of 280 nm, 210 nm, and 99 nm PS beads. All images were 2 µm x 2 µm.

When AFM data obtained from both methods with different PS particle diameters were considered, the films prepared from mono-layer 280 nm particles formed defect free highly ordered hexagonal packing both over small and large scales. The presence of step edges and nano-grooves were fully eliminated, as well as macroscopic non-ordered cracks. For these reasons, PLGA surfaces prepared from mono-layered 280 nm templates were selected for further characterization.

XPS and water contact angle measurements

Since chemistry, as well as topography, effect cell response to materials, XPS studies were carried out with the PLGA samples to determine whether the samples have similar chemistries after a hexane wash to reduce PDMS residuals. The studies were undertaken with textured and non-textured PLGA surfaces as well as a PLGA powder reference. XPS data indicated the presence of silicon at a similar thickness in textured (1.2 $\pm$ 0.3 nm) and non-textured (1.0 $\pm$ 0.1 nm) surfaces. (Table 1) This was assigned to PDMS oligomers carried over from the silicone mold. All other spectral features where equivalent in the textured and non-textured surfaces indicating chemical equivalence.

Table 1. XPS results, PDMS thickness calculations with and without topofactor correction, and contact angle measurements of the samples. The studies carried out with nanotextured PLGA films prepared from mono-layered 280 nm templates, and non-textured PLGA films after a hexane wash of the samples. For XPS studies, PLGA powder was also analyzed as a reference. The conformal coating thickness of PDMS was calculated using the stoichiometry of PDMS and a topofactor correction for the particle topography developed by Shard. (Shard *et al* 2009, Shard 2012)

	XPS results			**PDMS thickness (nm)**		**Contact angle *(θ)***
Samples	**C 1s %**	**O 1s %**	**Si 2p %**	**Non-corrected**	**Topofactor corrected**	

PLGA powder	62.9 ± 0.28	37.1 ± 0.28	_	_	_	_
Textured films	58.7 ± 2.44	33.1 ± 0.78	8.2 ± 1.9	1.6 ± 0.5	1.2 ± 0.3	104.4 ± 0.5
Non-textured films	63.2 ± 0.52	31.2 ± 0.51	5.6 ± 0.37	1.0 ± 0.1	_	107.9 ± 0.8

Overlayer PDMS thickness on PLGA particles were calculated from XPS data with the method described previously (Shard *et al* 2009). By using the topofactors given for the hemispheres, the equivalent conformal thickness was calculated via the thickness of PDMS as for a flat sample. According to the calculations, both flat samples and topofactor corrected textured surfaces have ~1 nm overlayer PDMS remaining. A two sample t-test was carried on the film PDMS film thicknesses and the P value was found to be 0.09, indicating that there was no statistical significance between the textured and non-textured films.

Contact angle measurements indicated that the wettability values of the surfaces were similar. In both surfaces, contact angle values were found higher than 90°, which indicates that the wetting of the surfaces were poor, and the surfaces were hydrophobic (Table 1).

Cell culture studies

OVCAR3 cells were studied in monoculture and in co-culture with MSC's in order to assess their response to 280 nm hemispherical topographies. Cell culture studies were carried out with PLGA surfaces prepared from mono-layered 280 nm templates and non-textured flat PLGA surfaces. Flat plate wells (tissue culture plastic only with no other added matrix/wafer/gel) were used for

control studies. OVCAR3, and OVCAR3 seeded with MSCs at a 1:1 ratio were cultured onto the surfaces. In the study, attachment of the cells to the films at 4th hour, 24th hour and 48th hour were studied.

OVCAR3 alone

It was observed that OVCAR3 cells were adhered to the surfaces by 4 hours and the mean number of cells attached per wafer were similar for both textured and non-textured surfaces but less than the flat plate well, cell culture plastic control (Figure 5, Figure S8, ESI).

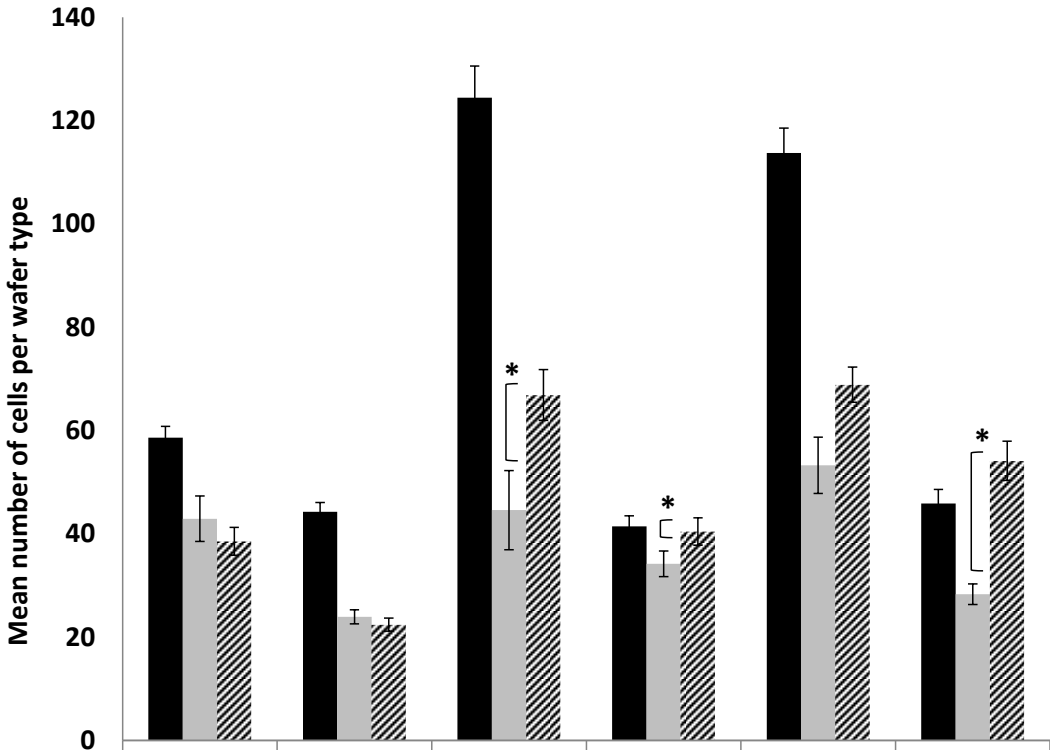

	4hrs OVCAR3	4hrs OVCAR3 with MSCs	24hrs OVCAR3	24hrs OVCAR3 with MSCs	48hrs OVCAR3	48hrs OVCAR3 with MSCs
flat plate well	58.63	44.27	124.46	41.42	113.75	45.88
non-textured surface	42.92	23.92	44.58	34.18	53.25	28.30
textured surface	38.54	22.42	66.88	40.43	68.89	54.13

Figure 5. Mean number of cells in OVCAR3 monocultures, and OVCAR3-MSC co-cultures per wafer type at 4h, 24h, and 48h. Flat well plates, non-textured PLGA surfaces, and PLGA

surfaces prepared from mono-layered 280 nm templates were used as a substrate. Data are expressed as a mean $\pm$ SD *: $p < 0.05$ compared to non-textured surfaces.

The mean number of cells per wafer increased for both textured and non-textured surfaces over time, however in the flat plate well cell culture control, a decrease was observed after 24 hours with OVCAR3's probably due to having reached confluency and then overgrowth of the cells on the well plate. The mean number of cells per wafer were higher on textured surfaces as compared to non-textured surfaces at the 24 and 48 hour time points and were significantly greater ($p < 0.05$) at the 24 hour time point. Also the cells at these time points were clustered in islets on the tissue culture plate control and wafers indicative of proliferation (Figure S8).

OVCAR3 co-cultured with MSCs

In the studies with OVCAR3 seeded 1:1 with MSC cell lines, again it was found that the cells were adhered to all surfaces by 4 hours and that the mean number of cells adhered per wafer were similar for both textured and non-textured surfaces but less than the flat plate well (Figure S9, ESI). Again, a decrease in the mean number of cells for the flat well plate at 24 hours was observed (Figure 5). The mean number of cells per wafer were significantly greater ($p < 0.05$) on textured surfaces as compared to the non-textured surface at 24 and 48 hour time points. Again, our results demonstrate that textured surfaces promote cell attachment compared to non-textured surfaces beyond the 4^{th} hour and also the cells at these time points were clustered in islets on the tissue culture plate control and wafers indicative of proliferation (Figure S9). .

DISCUSSION

There has been recent interest in the use of biomaterials to modulate cancer cell adhesion (Islam *et al* 2015, Hartman *et al* 2010, Kim *et al* 2013, Sharma *et al* 2014, Wan *et al* 2012) Motivated by the few studies in this area and to our knowledge none with ovarian cancer cells, we

investigated the modulation of ovarian cancer cell adhesion fabricating novel regularly nanotextured and defect-free materials over large lengths scales. Indeed, neither of these factors has been explored to date. Our first method of nanotexturing was to use a colloidal lithography approach similar to that reported by Zhang and Webster (Zhang and Webster 2012) where we observed with AFM, step edges in PLGA films as a result of formation of multi-layers during PS template preparation (Figures 2 and 3). These step-edges appear to be points of weakness in the interparticulate bonding, and resulted in PS particulate transfer to PDMS along these edges and subsequently PLGA films. Since it has been reported that cells can be aligned with surface features (known as "contact guidance") (Wilkinson *et al* 2002, Rajnicek *et al* 1997, Flemming *et al* 1999, Curtis and Wilkinson 1997), we then sort to find another colloidal lithography that could remove these features in the topography. Eliminating this response of the cells to non-ordered topography, allows study of cell response to nanotextured substrates only and to achieve this mono-layer PS templates were prepared. Monolayers of PS particles have been reported previously (Ogaki *et al* 2010), however here for the first time we used these to template nanotexture into PLGA surfaces for a biomaterial application. We found that we could create defect free nanotextured surfaces with nanotextured domes either 210 nm or 280 nm in diameter. However when smaller PS particle diameters were used in template preparation (99 nm and 57 nm), the order of small scale nanotexturing was disrupted. With this method, hexagonal packing is achieved by addition of SDS and indeed the particle diameters and SDS solution concentrations are crucial. Hence only the nanotextured surfaces with 280 nm nanotextured domes were progressed further where these films and a flat surface control were rigorously characterized using XPS and contact angle measurements. These measurements proved chemical

equivalence in surface chemistry and hence we can be certain that any difference in cell response is due to topography i.e. nanotexturing.

Using these 280 nm nanotextured defect free films and a flat surface control of chemical equivalence, we then progressed to evaluating OVCAR3 cell adhesion on these films, in monoculture and in co-culture with MSCs. Our data shows that OVCAR3 cell adhesion, whether in monoculture or co-cultured with MSCs, to all surfaces and similarities between textured and non-textured surfaces at the four hour time point as also reported by Zhang and Webster (Zhang and Webster 2012) for breast cancer cells. It should also be noted that these cell attachment studies are also the first to our knowledge using a co-culture with MSCs.

However at 24 and 48 hour time points, our results demonstrated that textured surfaces have more cells attached compared to non-textured surfaces when alone or co-cultured with MSCs. Our data is in agreement with previous studies with cell lines where reported changes in cell attachment were observed compared to non-textured surfaces. In some papers, a decrease in cell adhesion/proliferation was reported due to texturing (Wilkinson *et al* 2002, Curtis *et al* 2001), and oppositely some reported an increase in cell adhesion/proliferation (Miller *et al* 2007, Carpenter *et al* 2008) as was observed in our studies.

CONCLUSIONS

In this study, we aimed to investigate the effect of hemispherical protrusion surface topographies on ovarian cancer cell adhesion. For this purpose, flat and nanotextured PLGA films obtained from (1) mono-layered and (2) multi-layered PS templates were characterized by AFM and optical microscope.

According to our results:

- Films obtained from multi-layered templates had non-ordered, uncontrolled surface topographies (macroscopic structures and step edges).
- Films obtained from monolayered templates were defect-free at large length scales, and demonstrated nanotexturing in small scale. However it was found that when the PS particle diameters for template preparation decreased to 99 nm and 57 nm, the order of small scale nanotexturing was disrupted.
- Whilst in the cancer cell adhesion studies, OVCAR3 seeded alone, and seeded with MSCs, cancer cells adhered to all surfaces, and increased cell numbers on textured surfaces compared with the non-textured surfaces was observed at 24 and 48 hour time points.

ASSOCIATED CONTENT

Supporting Information. Control studies for the films with AFM and optical microscope, AFM section analysis of 280 nm PDMS templates, AFM topography images of surfaces with the scan sizes of 8 μm x 8 μm, AFM topography images of PS surfaces prepared from mono-layer 57 nm PS templates. Optical microscope images of OVCAR3 and MSC cell adhesion on flat well, non-textured surface and textured surface at 4 hrs, 24 hrs, and 48 hrs. This material is available free of charge via the Internet at http://pubs.acs.org

AUTHOR INFORMATION

Corresponding Author

* E-mail: Maria.Marlow@nottingham.ac.uk

Author Contributions

The manuscript was written through contributions of all authors. All authors have given approval to the final version of the manuscript.

Funding Sources

This research is funded by EPSRC Research Development Fund, Grant: Call–RDF-PP-0313.

Notes

The authors declare no competing financial interest.

ACKNOWLEDGMENT

Thanks to Dr Ryosuke Ogaki for his help in preparation of mono-layer PS templates, Taranjit Singh for water contact angle measurements. Thanks to Dr Emily Smith at the Nottingham Nanotechnology and Nanoscience Centre for performing the XPS analysis and EPSRC for funding the XPS instrument, Grant EP/K005138/1. Thanks go to Alex G. Shard at the National Physical Laboratory for his help on the XPS topofactor analysis.

ABBREVIATIONS

AFM, atomic force microscopy; DMEM, Dulbecco's modified eagles medium; ECM, extracellular matrix; FAT, fixed analyzed transmission; FBS, Fetal bovine serum; MSC, mesenchymal stem cell; OVCAR3, human ovarian cancer cell; PDMS, polydimethylsiloxane; PLGA, poly(lactic-co-glycolic acid); PS, polystyrene; SDS, dodecylsodiumsulfate; XPS, X-ray photoelectron spectroscopy.

REFERENCES

Andersson A S, Backhed F, von Euler A, Richter-Dahlfors A, Sutherland D and Kasemo B 2003 Nanoscale features influence epithelial cell morphology and cytokine production *Biomaterials* **24** 3427-36

Carpenter J, Khang D and Webster T J 2008 Nanometer polymer surface features: the influence on surface energy, protein adsorption and endothelial cell adhesion *Nanotechnology* **19**

Craighead H G, Turner S W, Davis R C, James C, Perez A M, St John P M, Isaacson M S, Kam L, Shain W, Turner J N and Banker G 1998 Chemical and Topographical Surface Modification for Control of Central Nervous System Cell Adhesion *Biomedical Microdevices* **1** 49-64

Curtis A and Wilkinson C 1997 Topographical control of cells *Biomaterials* **18** 1573-83

Curtis A S G, Casey B, Gallagher J O, Pasqui D, Wood M A and Wilkinson C D W 2001 Substratum nanotopography and the adhesion of biological cells. Are symmetry or regularity of nanotopography important? *Biophysical Chemistry* **94** 275-83

Dalby M J, Giannaras D, Riehle M O, Gadegaard N, Affrossman S and Curtis A S G 2004 Rapid fibroblast adhesion to 27 nm high polymer demixed nano-topography *Biomaterials* **25** 77-83

Falconnet D, Csucs G, Grandin H M and Textor M 2006 Surface engineering approaches to micropattern surfaces for cell-based assays *Biomaterials* **27** 3044-63

Flemming R G, Murphy C J, Abrams G A, Goodman S L and Nealey P F 1999 Effects of synthetic micro- and nano-structured surfaces on cell behavior *Biomaterials* **20** 573-88

Haller D, Bode C, Hammes W P, Pfeifer A M A, Schiffrin E J and Blum S 2000 Non-pathogenic bacteria elicit a differential cytokine response by intestinal epithelial cell/leucocyte co-cultures *Gut* **47** 79-87

Hartman O, Zhang C, Adams E L, Farach-Carson M C, Petrelli N J, Chase B D and Rabolt J E 2010 Biofunctionalization of electrospun PCL-based scaffolds with perlecan domain IV peptide to create a 3-D pharmacokinetic cancer model *Biomaterials* **31** 5700-18

Hsu S H, Chen C Y, Lu P S, Lai C S and Chen C J 2005 Oriented Schwann cell growth on microgrooved surfaces *Biotechnology and Bioengineering* **92** 579-88

Islam M, Sajid A, Mahmood M A I, Bellah M M, Allen P B, Kim Y T and Iqbal S M 2015 Nanotextured polymer substrates show enhanced cancer cell isolation and cell culture *Nanotechnology* **26**

Kim H N, Jiao A, Hwang N S, Kim M S, Kang D H, Kim D H and Suh K Y 2013 Nanotopography-guided tissue engineering and regenerative medicine *Advanced Drug Delivery Reviews* **65** 536-58

Lamers E, Walboomers X F, Domanski M, te Riet J, van Delft F, Luttge R, Winnubst L, Gardeniers H and Jansen J A 2010 The influence of nanoscale grooved substrates on osteoblast behavior and extracellular matrix deposition *Biomaterials* **31** 3307-16

Lehmann A D, Daum N, Bur M, Lehr C-M, Gehr P and Rothen-Rutishauser B M 2011 An in vitro triple cell co-culture model with primary cells mimicking the human alveolar epithelial barrier *European Journal of Pharmaceutics and Biopharmaceutics* **77** 398-406

Martinez E, Engel E, Planell J A and Samitier J 2009 Effects of artificial micro- and nano-structured surfaces on cell behaviour *Annals of Anatomy-Anatomischer Anzeiger* **191** 126-35

Matsuzaka K, Walboomers X F, Yoshinari M, Inoue T and Jansen J A 2003 The attachment and growth behavior of osteoblast-like cells on microtextured surfaces *Biomaterials* **24** 2711-9

Miller D C, Haberstroh K M and Webster T J 2007 PLGA nanometer surface features manipulate fibronectin interactions for improved vascular cell adhesion *Journal of Biomedical Materials Research Part A* **81A** 678-84

Ng R, Zang R, Yang K K, Liu N and Yang S-T 2012 Three-dimensional fibrous scaffolds with microstructures and nanotextures for tissue engineering *Rsc Advances* **2** 10110-24

Ogaki R, Lyckegaard F and Kingshott P 2010 High-Resolution Surface Chemical Analysis of a Trifunctional Pattern Made by Sequential Colloidal Shadowing *Chemphyschem* **11** 3609-16

Rajnicek A M, Britland S and McCaig C D 1997 Contact guidance of CNS neurites on grooved quartz: influence of groove dimensions, neuronal age and cell type *Journal of Cell Science* **110** 2905-13

Recknor J B, Recknor J C, Sakaguchi D S and Mallapragadaa S K 2004 Oriented astroglial cell growth on micropatterned polystyrene substrates *Biomaterials* **25** 2753-67

Rybczynski J, Ebels U and Giersig M 2003 Large-scale, 2D arrays of magnetic nanoparticles *Colloids and Surfaces a-Physicochemical and Engineering Aspects* **219** 1-6

Sarna M, Wybieralska E, Miekus K, Drukala J and Madeja Z 2009 Topographical control of prostate cancer cell migration *Molecular Medicine Reports* **2** 865-71

Shard A G 2012 A Straightforward Method For Interpreting XPS Data From Core-Shell Nanoparticles *Journal of Physical Chemistry C* **116** 16806-13

Shard A G, Wang J and Spencer S J 2009 XPS topofactors: determining overlayer thickness on particles and fibres *Surface and Interface Analysis* **41** 541-8

Sharma A, Sharma N L, Lavy C B, Kiltie A E, Hamdy F C and Czernuszka J 2014 Three-dimensional scaffolds: an in vitro strategy for the biomimetic modelling of in vivo tumour biology *Journal of Materials Science* **49** 5809-20

Touboul C, Lis R, Al Farsi H, Raynaud C M, Warfa M, Althawadi H, Mery E, Mirshahi M and Rafii A 2013 Mesenchymal stem cells enhance ovarian cancer cell infiltration through IL6 secretion in an amniochorionic membrane based 3D model *Journal of Translational Medicine* **11**

Wan Y, Mahmood M A I, Li N, Allen P B, Kim Y T, Bachoo R, Ellington A D and Iqbal S M 2012 Nanotextured substrates with immobilized aptamers for cancer cell isolation and cytology *Cancer* **118** 1145-54

Wilkinson C D W, Riehle M, Wood M, Gallagher J and Curtis A S G 2002 The use of materials patterned on a nano- and micro-metric scale in cellular engineering *Materials Science & Engineering C-Biomimetic and Supramolecular Systems* **19** 263-9

Zhang L and Webster T J 2012 Poly-lactic-glycolic-acid surface nanotopographies selectively decrease breast adenocarcinoma cell functions *Nanotechnology* **23**

Table of Contents Graphic and Synopsis

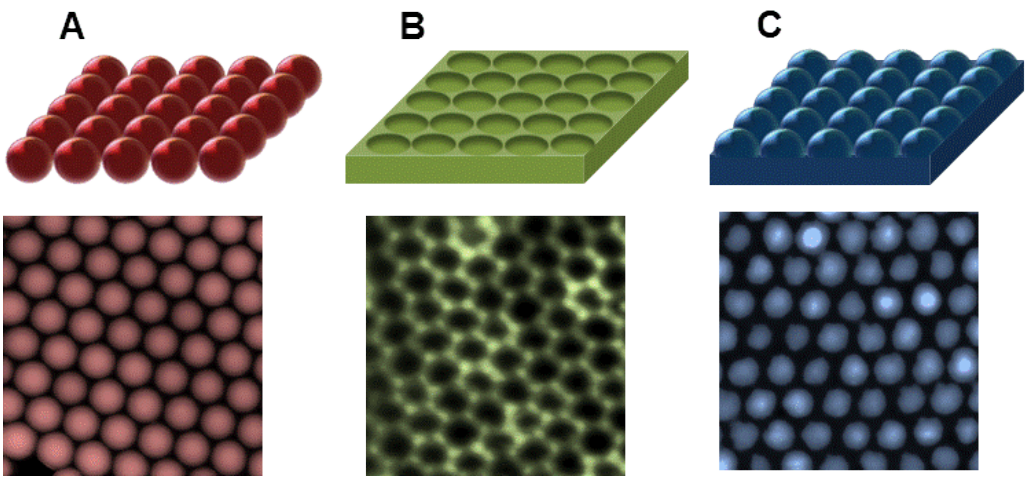

Hemispherical protrusion shaped nanotextured materials were manufactured using a colloidal particle lithography technique and characterized using AFM. Cell attachment of a human ovarian cancer cell line (OVCAR3) on these nano-patterned surfaces was greater as compared to a flat, non-textured control for 24 and 48 hour time points A schematic representation of the colloidal particle lithography technique and associated AFM images: Polystyrene surfaces (A), polydimethylsiloxane surfaces (B), and poly(lactic-co-glycolic acid) surfaces (C).